THE CALCULATION OF THE VIBRATION–ROTATION ENERGIES OF TRIATOMIC MOLECULES USING SCATTERING COORDINATES

Jonathan TENNYSON

Department of Physics and Astronomy, University College London, Gower Street,
London WC1E 6BT, England

1986

NORTH-HOLLAND – Amsterdam

Contents

Computer Physics Reports 4 (1986) 1–36
North-Holland, Amsterdam

THE CALCULATION OF THE VIBRATION–ROTATION ENERGIES OF TRIATOMIC MOLECULES USING SCATTERING COORDINATES

Jonathan TENNYSON

Department of Physics and Astronomy, University College London, Gower Street, London WC1E 6BT, England

Received 25 January 1986

This paper is a review of work I have been involved with concerning the calculation of ro–vibrational energy levels and wavefunctions, mainly of triatomic systems. The method reviewed is that of Tennyson and Sutcliffe for the calculation of spectra of triatomics as atom–diatom collision complexes, which is particularly appropriate for molecules with one or more large amplitude vibrational mode. The method uses polynomial basis functions to carry the nuclear motions and is variational for a given potential. Hamiltonians for four different sets of body-fixed axes are derived. The computational implementation of the method is discussed, including improvements to some published algorithms. The use of a two step (secondary) variational procedure for highly-excited rotational states is discussed and sample results given. Extensions to non-Born–Oppenheimer problems, transition intensities and polyatomic molecules are also considered. Comparisons are made with other techniques for calculating ro–vibrational spectra with some specific molecular examples.

1. Introduction

The parallel improvements in the laser and computer technology since 1970 have given great impetus to the calculation of molecular vibration–rotation spectra. These improvements have lead to potential energy surfaces, both empirical and theoretical, which can be used to perform nuclear motion calculations yielding observables. Indeed, since experimental spectra cannot in general be directly inverted to give potential energy surfaces, it is only through the computation and comparison with experiment of spectroscopic and other properties that these surfaces can be systematically tested and improved. Such calculations can of course also be used predictively to aid the observation and assignment of transitions.

For a given potential, the calculation of simple diatomic vibration–rotation energy levels can easily be achieved by direct integration of the corresponding one-dimensional Schrödinger equation [1]. Conversely, the $3N-6$ coupled differential equations which are implied for the complete solution of the non-linear polyatomic vibrational problem are currently intractable even for medium ($N > 4$) size N-atomic molecules, without approximations which lead to significant decoupling. The commonest of these are the well-known harmonic approximation [2] and the freezing of selected vibrational modes, usually on the grounds of energy separation or mode localisation [3]. Between these extremes, triatomic, and more recently tetra-atomic, molecules have proved a fruitful testing ground where a variety of ro–vibrational methods can be tried on challenging and interesting problems.

The necessity of removing translational motion and the desirability of identifying rotational motions leads to some flexibility in the choice of a Hamiltonian for a given ro–vibrational problem. The Hamiltonian and solution strategy chosen for a particular calculation thus in some way reflect one's physical insight into the problem.

Most of the early treatments of triatomics, such as the still [4] popular water molecule, used the Eckart conditions [5] and were expressed in displacement coordinates from some equilibrium structure [6]. Perhaps the pick of these methods is that due to Whitehead and Handy [7,8]; it uses Watson's Hamiltonian [9], harmonic oscillator functions (weighted Hermite polynomials) as a basis to carry the nuclear motions and Gauss–Hermite quadrature to do the integrals. Diagonalisation of the resulting secular problem leads to results for a potential which are, in principle, exact within the usual confines of the variational principle. This and related methods have been used successfully for several triatomics [4,6,10,11] and with more difficulty, because of the demands of the numerical integration, for tetra-atomics [12–14]. However, experience with floppy molecules, in particular KCN [15–17] and CH_2^+ [18–22], showed that this approach can give spurious results. The problems are twofold. Firstly, the Watson term in the Hamiltonian for bent molecules is singular for linear geometries as the Hamiltonian does not go smoothly from one with $3N-6$ to one with $3N-5$ vibrational modes [23]. Secondly, with the numerical procedures outlined above it is possible to leave the true domain of the problem [4,24]. More generally, methods based on displacements from some equilibrium geometry are not necessarily appropriate for large amplitude modes for which the concept of a special geometry is not useful.

It is possible to build a do-it-yourself Hamiltonian simply by defining a suitable set of internal coordinates and a suitable orientation for the axes. This process of coordinate transformation is known as embedding. As any coordinate choice will, in general, give rise to singularities in the Hamiltonian, the coordinates and hence the Hamiltonian that one chooses to represent a vibrational problem should be dictated by the potential of that problem [25]. As a response to the difficulties encountered with the Hamiltonian based on the Eckart conditions, the idea of developing Hamiltonians using the recipe of Sutcliffe [26], appropriate to each class of problems has arisen [21,22,27]. This has the advantage that in each case a physically motivated coordinate system can be used, but has the drawback that, especially as larger molecules are tackled, a proliferation of Hamiltonians and solution techniques will necessarily result. Furthermore, the algebra involved in deriving these Hamiltonians can be complicated with at least one case of acknowledged defeat having already appeared in the literature [28].

An alternative approach to the problem of large amplitude vibrational motion is through (approximate) mode separation. Thus the (semi-, non-) rigid bender method finds accurate solutions only for a single low energy (large amplitude) coordinate, allowing only partially for the relaxation of the other coordinates. This method, which originated with Sayvetz [29], has recently been reviewed by Bunker [30] and Jensen [31]. A complimentary approach, which considers only the high energy, small amplitude coordinates, has been employed by Botschwina [32].

In the same spirit as these are methods based on a Born–Oppenheimer-like separation between low and high frequency vibrational modes [33–38]. The widest used of these is the BOARS (Born–Oppenheimer Angular Radial Separation) approximation, which solves successively for low and high energy modes [33–35]. These methods have found considerable success for molecules where such mode separation is appropriate. Their computational speed has allowed both the nonrigid bender method [39–41] and the BOARS approximation [42,43] to be used iteratively to produce semi-empirical potentials. However, for many molecules there is no appropriate mode separation. Indeed, recent work has suggested that, particularly for highly excited vibrational states, such mode separation can lead to qualitatively incorrect results [44,45].

This paper considers an approach to bound state ro–vibrational calculations whose origins lie in heavy particle scattering and in particular in the close-coupled equations of Arthurs and Dalgarno [46]. Instead of concentrating on a single mode, the method allows for the large amplitude motion of $\boldsymbol{R}$ the vector connecting the centre of mass of two fragments. For a triatomic, this means the motion of an atom relative to a diatom. The internal coordinates of the fragment. The diatom in the triatomic example, may also be treated at the same time or in some alternative, approximate fashion. This coordinate representation is appropriate, in the potential driven sense of Sutcliffe [25], to the interactions of a Van der Waals complex, but methods based on it have proved robust enough to give accurate results for systems which bear little or not resemblance to Van der Waals complexes.

This paper will consider the formalism underlying the bound state close-coupling method as well as strategies and numerical procedures which have been employed for its solution, concentration particularly on the secular matrix approach of Tennyson and Sutcliffe [17,20,47]. The method is not represented by a single computer program as different variants have been used for different problems. However references will be provided to published programs and it is hoped that the article will prove useful to a reader wishing to tackle a specific problem using this methodology. Some applications will also be discussed, without aiming for a comprehensive survey, so that the effectiveness of the method may be judged. Finally, extensions of the method to dipole dependent properties, such as intensities, and Born–Oppenheimer breakdown will also be briefly considered.

2. The Hamiltonian

2.1. Space-fixed coordinates

In this chapter the Hamiltonian representing the nuclear motion of triatomic systems will be considered. A generalisation of the Hamiltonian to the interaction of two polyatomic fragments has been given by Brocks et al. [48]. However, this Hamiltonian in its most general form has yet to be used for computational work. This article will largely be concerned with triatomic systems, although some larger calculations, notably diatom–diatom [49] and atom–polyatom [50] will also be discussed.

Within the Born–Oppenheimer approximation, the Hamiltonian for the motion of three atoms is

$$H = -\frac{\hbar}{2} \sum_{i=1}^{3} \frac{1}{m_i} \nabla^2(\boldsymbol{x}_i) + V, \tag{2.1}$$

where $\nabla^2(\boldsymbol{x}_i)$ is the Laplacian for the ith nucleus, which has mass m_i, and V is the electronic potential, which depends only on the relative (or internal) nuclear coordinates. The first step in the construction of any ro–vibrational Hamiltonian is the removal of the overall translational motion. To do this a new set of coordinates may be defined

$$\begin{aligned} \boldsymbol{R} &= \boldsymbol{x}_1 - \boldsymbol{x}_\mathrm{d}, \\ \boldsymbol{r} &= \boldsymbol{x}_3 - \boldsymbol{x}_2, \\ \boldsymbol{X} &= M^{-1} \sum_{i=1}^{3} m_i \boldsymbol{x}_i, \end{aligned} \tag{2.2}$$

where

$$\begin{aligned} m_\mathrm{d} &= m_2 + m_3, \\ M &= m_1 + m_\mathrm{d}, \\ \boldsymbol{x}_\mathrm{d} &= m_\mathrm{d}^{-1}(m_2 \boldsymbol{x}_2 + m_3 \boldsymbol{x}_3). \end{aligned} \tag{2.3}$$

$\boldsymbol{r}$ is the diatom bond vector and $\boldsymbol{R}$ is the vector connecting the diatom centre of mass with the atom. The centre of mass of the whole complex is given by $\boldsymbol{X}$.

Use of the chain rule gives

$$\sum_{i=1}^{3} \frac{1}{m_i} \nabla^2(\boldsymbol{x}_i) = M^{-1}\, \nabla^2(\boldsymbol{X}) + \mu^{-1}\, \nabla^2(\boldsymbol{R}) + \mu_\mathrm{d}^{-1}\, \nabla^2(\boldsymbol{r}), \tag{2.4}$$

with

$$\begin{aligned} \mu_\mathrm{d} &= m_2^{-1} + m_3^{-1}, \\ \mu &= m_1^{-1} + m_\mathrm{d}^{-1}. \end{aligned} \tag{2.5}$$

Removing the centre of mass motion and expanding the Laplacian operators, one reaches the familiar space-fixed Hamiltonian [16,51,52]

$$H = -\frac{\hbar^2}{2\mu R}\frac{\partial^2}{\partial R^2}R - \frac{\hbar^2}{2\mu_\mathrm{d} r}\frac{\partial^2}{\partial r^2}r + \frac{\boldsymbol{l}^2}{2\mu R^2} + \frac{\boldsymbol{j}^2}{2\mu_\mathrm{d} r^2} + V, \tag{2.6}$$

where $\boldsymbol{l}$ and $\boldsymbol{j}$ are angular momentum operators whose eigenfunctions are spherical harmonics in the polar angles $\hat{R}$ and $\hat{r}$, respectively. The total angular momentum operator is given by the vector sum of the angular momentum of the diatom, $\boldsymbol{j}$, and that of the complex, $\boldsymbol{l}$.

$$\boldsymbol{J} = \boldsymbol{l} + \boldsymbol{j}. \tag{2.7}$$

The Jacobian in (2.6) and subsequent Hamiltonians is $R^2 r^2 \sin\theta$, where θ is the angle between $\boldsymbol{r}$ and $\boldsymbol{R}$. It has been taken to the left of the operator as this simplifies the form of the radial kinetic energy operators. Matrix elements over these Hamiltonians and other operators will be written $\langle i, j \,|\, \hat{O} \,|\, i', j' \rangle$, where it will be assumed that the integration is performed only over the coordinates for which the basis set is explicitly given, i and j in the example, and that the relevant portion of the Jacobian is included from the left.

2.2. Body-fixed coordinates

Although the space-fixed representation has been successfully used for several ro–vibrational calculations, it is generally desirable to work with a body-fixed frame. This frame has the advantage that vibrational and rotational coordinates can easily be identified, along with the Coriolis terms which couple them and that the resulting close-coupled equations are simpler than those derived from the space-fixed Hamiltonian.

However, even within the restricted coordinate system considered here, there is no unique way of fixing the axes to the coordinate frame. Four ways of doing this, embedding, will be considered. At least three of these representations have been used for actual calculations [17,53,54]. The computational equivalence, for a suitable choice of angular basis functions, between the two- and three-angle embeddings will be demonstrated, while examples favouring the use of both $\boldsymbol{r}$ and $\boldsymbol{R}$ embeddings will be given.

The problem of embedding the coordinates in the general polyatomic Hamiltonian has been considered by Brocks et al. [45]. They showed that the two-angle embedding implied by rotating $\boldsymbol{R}$ to lie along the z-axis and leaving the third Euler angle undefined gave the most satisfactory general Hamiltonian. Embedding the third angle gives a Hamiltonian which is inconvenient for systems larger than triatomic.

For triatomics, however, embeddings which place the z-axis along $\boldsymbol{r}$ as well as the more usual $\boldsymbol{R}$ embedding have been used [20,53]. Considering first the two-angle embedding one can define an orthogonal transformation

$$z = \mathbf{C}^\mathrm{T} \boldsymbol{t}, \tag{2.8}$$

where for the $\boldsymbol{R}$ embedding

$$\boldsymbol{t}=\boldsymbol{R}, \quad z=\begin{pmatrix}0\\0\\R\end{pmatrix}, \quad \hat{R}=(\beta,\alpha) \tag{2.9}$$

and for the $\boldsymbol{r}$ embedding

$$\boldsymbol{t}=\boldsymbol{r}, \quad z=\begin{pmatrix}0\\0\\r\end{pmatrix}, \quad \hat{r}=(\beta,\alpha), \tag{2.10}$$

where, of course, the Euler angles for the two embeddings are not equivalent. The orthogonal matrix $\mathbf{C}$ is given by

$$\mathbf{C}=\begin{pmatrix}\cos\beta\cos\alpha & -\sin\beta & \sin\beta\cos\alpha\\ \cos\beta\sin\alpha & \cos\beta & \sin\beta\sin\alpha\\ -\sin\beta & 0 & \cos\beta\end{pmatrix}, \tag{2.11}$$

The kinetic energy operator in the new coordinates can be obtained by use of the chain rule,

$$K=-\frac{\hbar^2}{2\mu R}\frac{\partial^2}{\partial R^2}R-\frac{\hbar^2}{2\mu_{\mathrm{d}}r}\frac{\partial^2}{\partial r^2}r+\frac{1}{2\mu_1 v_1^2}\left[J^2+j^2-2\boldsymbol{j}\cdot\boldsymbol{J}\right]+\frac{1}{2\mu_2 v_2^2}j^2, \tag{2.12}$$

where J^2 has the unusual form [48,54]

$$J^2=J_x^2+\operatorname{cosec}\beta J_y\sin\beta J_y+J_z^2 \tag{2.13}$$

which means that $\boldsymbol{J}$ and $\boldsymbol{j}$ do not commute and

$$(\boldsymbol{J}-\boldsymbol{j})^2=\left[J^2+j^2-2\boldsymbol{j}\cdot\boldsymbol{J}\right]=\left[J^2+j^2-2j_zJ_z-j_+J_+-j_-J_-\right]. \tag{2.14}$$

For the $\boldsymbol{R}$ embedding

$$\mu_1=\mu, \quad v_1=R; \quad \mu_2=\mu_{\mathrm{d}}, \quad v_2=r \tag{2.15}$$

and for the $\boldsymbol{r}$ embedding

$$\mu_1=\mu_{\mathrm{d}}, \quad v_1=r; \quad \mu_2=\mu, \quad v_2=R. \tag{2.16}$$

For the $\boldsymbol{R}$ embedding, this form of the Hamiltonian is well known [52,54].

For triatomics it is often convenient to body-fix all three Euler angles. Starting from the two-angle embedding given above, embedding $\boldsymbol{R}$ placed $\boldsymbol{R}$ along the z-axis and $\boldsymbol{r}$ in the x–y plane and was the one originally chosen by Tennyson and Sutcliffe [17]; while embedding $\boldsymbol{r}$, of Istomin et al. [53] places $\boldsymbol{r}$ along z and $\boldsymbol{R}$ in the x–y plane. Fig. 1 illustrates the embeddings. With either orientation of the axes the Hamiltonian has the form

$$H=K_{\mathrm{V}}+K_{\mathrm{VR}}+V(R,r,\theta), \tag{2.17}$$

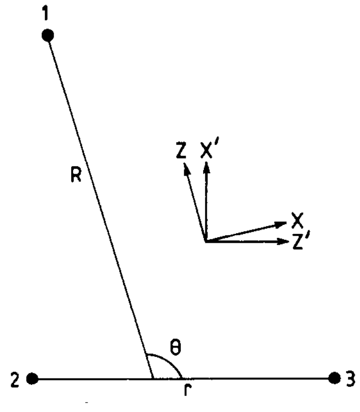

Fig. 1. Coordinate system: (x, z) are the axes for the $\boldsymbol{R}$ embedding and (x', z') are for the $\boldsymbol{r}$ embedding.

where the vibrational kinetic energy operator is analogous to the two-angle embedded one discussed above

$$K_{\mathrm{V}} = -\frac{\hbar^2}{2\mu R}\frac{\partial^2}{\partial R^2}R - \frac{\hbar^2}{2\mu_{\mathrm{d}} r}\frac{\partial^2}{\partial r^2}r - \frac{\hbar^2}{2}\left(\frac{1}{\mu R^2} + \frac{1}{\mu_{\mathrm{d}} r^2}\right)\frac{1}{\sin\theta}\frac{\partial}{\partial\theta}\left(\sin\theta\frac{\partial}{\partial\theta}\right), \tag{2.18}$$

and the vibration–rotation kinetic energy operator depends on the embedding chosen

$$\begin{aligned} K_{\mathrm{VR}} = \frac{1}{2}&\left[\frac{1}{\mu_1 v_1^2}\left(\Pi_x^2 + \Pi_y^2\right) + \left(\frac{\cot^2\theta}{\mu_1 v_1^2} + \frac{\operatorname{cosec}^2\theta}{\mu_2 v_2^2}\right)\Pi_z^2\right] \\ &+ \frac{\cot\theta}{2\mu_1 v_1^2}\left(\Pi_x\Pi_z + \Pi_z\Pi_x\right) + \frac{\hbar}{i}\frac{1}{\mu_1 v_1^2}\left(\frac{\partial}{\partial\theta} + \frac{\cot\theta}{2}\right)\Pi_y, \end{aligned} \tag{2.19}$$

where Π_i are the components of the total angular momentum chosen to satisfy the usual commutation relations [17]. It is worth noting that K_{VR}, in contrast to K_{V}, is singular for $\theta = 0$, i.e. for linear molecular geometrics. This point will be developed when the choice of angular basis functions is discussed in the following section.

3. Solution strategy

3.1. Angular basis functions

In space-fixed coordinates a complete angular basis for the triatomic problem can be written [16,51]

$$\mathcal{Y}_{j,l}^{J,M} = \sum_{m=-j}^{j} Y_{j,m}(\hat{R})Y_{l,M-m}(\hat{r})\langle J, M \mid j, m;\ l, M-m\rangle, \tag{3.1}$$

where the spherical harmonics and Clebsch–Gordan coefficients are conventional [55] and $\hat{a}$ is used to represent the polar angles of vector $\boldsymbol{a}$. The coupling ensures that the basis functions have the correct total angular momentum quantum numbers, J and M. It is also possible to work with uncoupled functions [43].

Transforming these functions to the two-angle body-fixed frame gives

$$\mathscr{Y}_{j,q}^{J,M} = Y_{j,q}(\theta, \gamma)\mathscr{D}_{M,q}^{J*}(\alpha, \beta, 0), \tag{3.2}$$

where the rotation matrix, $\mathscr{D}_{M,q}^{J}$, is defined according to Brink and Satchler [55]. q is the projection of the total angular momentum J on the body-fixed axis. By convention this projection is usually denoted k for the $\boldsymbol{R}$ embedding and Ω for the $\boldsymbol{r}$ embedding [20].

If all three Euler angles are used to body-fix the coordinate frame, the angular basis becomes

$$\mathscr{Y}_{j,q}^{J,M} = \Theta_{j,q}(\theta)\mathscr{D}_{M,q}^{J*}(\alpha, \beta, \gamma), \tag{3.3}$$

where $\Theta_{j,q}$ is an associated Legendre polynomial with the phase conventions of Condon and Shortley [56]. However, as has been noted before [17], the relationship

$$\Theta_{jq}(\theta)\mathscr{D}_{M,q}^{J*}(\alpha, \beta, \gamma) = Y_{j,q}(\theta, \gamma)\mathscr{D}_{M,q}^{J*}(\alpha, \beta, 0) \tag{3.4}$$

means that the angular functions of eqs. (3.2) and (3.3) are equivalent.

The action of the angular momentum operators discussed above on these body-fixed functions gives (in the two angle embedding)

$$j^2\mathscr{Y}_{j,q}^{J,M} = \hbar^2 j(j+1)\mathscr{Y}_{j,q}^{J,M}, \tag{3.5}$$

$$J^2\mathscr{Y}_{j,q}^{J,M} = \hbar^2 J(J+1)\mathscr{Y}_{j,q}^{J,M}, \tag{3.6}$$

$$j_z J_z \mathscr{Y}_{j,q}^{J,M} = \hbar^2 q^2 \mathscr{Y}_{j,q}^{J,M}, \tag{3.7}$$

$$j_\pm J_\pm \mathscr{Y}_{j,q}^{J,M} = \hbar^2 C_{j,q}^{\pm} C_{J,q}^{\pm} \mathscr{Y}_{j,q\pm1}^{J,M}, \tag{3.8}$$

where

$$C_{l,q}^{\pm} = [l(l+1) - q(q\pm1)]^{1/2}. \tag{3.9}$$

Letting the appropriate body-fixed Hamiltonian (see eq. (2.12)) act on these basis functions, multiplying from the left by their complex conjugate and integrating over all angular coordinates gives the operator

$$\begin{aligned} H_{j,q,j'q'}^{J,M} = \hbar^2 \delta_{j,j'}\delta_{q,q'}\Bigg[& -\frac{1}{2\mu R}\frac{\partial^2}{\partial R^2}R - \frac{1}{2\mu_{\mathrm{d}} r}\frac{\partial^2}{\partial r^2}r + j(j+1) \\ & \times\left(\frac{1}{2\mu R^2} + \frac{1}{2\mu_{\mathrm{d}} r^2}\right) + \frac{J(J+1) - 2q^2}{2\mu_1 v_1^2}\Bigg] \\ & -\delta_{j,j'}\frac{\hbar^2}{2\mu_1 v_1^2}\left[C_{J,q}^{+}C_{j,q}^{+}\delta_{q',q+1} + C_{J,q}^{-}C_{j,q}^{-}\delta_{q',q-1}\right] + \langle j', q' | V | j, q\rangle \end{aligned} \tag{3.10}$$

which in turn gives the well-known close-coupled equations [46]. This operator is identical to the one given by using the three-angle embedding (2.17) and angular functions (3.3).

Unlike the three-angle embedded Hamiltonian of eqs. (2.17)–(2.19), the operator $H^{J,M}_{j,q,j',q'}$ is not singular for $\theta = 0$. This is because the explicit coupling of the vibrational, $\Theta_{j,q}(\theta)$, and rotational, $\mathscr{D}^{J*}_{M,q}(\alpha, \beta, \gamma)$, functions through the common index q leads to a cancellation between the singular terms arising from the last term in (2.18) and (2.19). Physically, this coupling allows for the smooth transition from a bent system with 3 rotational degrees of freedom to a linear one with 2 rotational degrees of freedom. In this sense the two-angle embeddings are appropriate for linear molecules and the three-angle embeddings for bent ones. However, as the equivalence of the two approaches has been demonstrated, at least for triatomics, no distinction will be drawn between them in the following discussion. Conversely, all polyatomic calculations have so far relied on the two-angle $\boldsymbol{R}$ embedding [48–50].

3.2. The potential

In the usual formulation of the close-coupled equations, the potential is assumed to be represented by a Legendre expansion

$$V(R, r, \theta) = \sum_{\lambda} V_{\lambda}(R, r) P_{\lambda}(\cos\theta). \tag{3.11}$$

If this is so, the angular integration over the potential can be performed analytically. In space-fixed coordinates

$$\langle \mathscr{Y}^{J,M}_{j,l} \,|\, V \,|\, \mathscr{Y}^{J,M}_{j',l'} \rangle = \sum_{\lambda} f_{\lambda}(j, l, j', l'; J) V_{\lambda}(R, r), \tag{3.12}$$

where $f_{\lambda}(j, l, j', l'; J)$ are Percival–Seaton coefficients [57] given by

$$f_{\lambda}(j, l, j', l'; J) = (-1)^{j'+l+J} [(2j+1)(2j'+1)(2l+1)(2l'+1)]^{1/2} \times \begin{pmatrix} j' & \lambda & j \\ 0 & 0 & 0 \end{pmatrix} \begin{pmatrix} l' & \lambda & l \\ 0 & 0 & 0 \end{pmatrix} \begin{Bmatrix} J & l & j \\ \lambda & j' & l' \end{Bmatrix} \tag{3.13}$$

using the usual $3-j$ and $6-j$ symbols [55]. In body-fixed coordinates

$$\langle j, q \,|\, V \,|\, j', q' \rangle = \delta_{q,q'} \sum_{\lambda} g_{\lambda}(j, j', q) V_{\lambda}(R, r), \tag{3.14}$$

where $g_{\lambda}(j, j', q)$ are Gaunt coefficients [58]

$$g_{\lambda}(j, j', q) = (-1)^{q} [(2j+1)(2j'+1)]^{1/2} \begin{pmatrix} j' & \lambda & j \\ 0 & 0 & 0 \end{pmatrix} \begin{pmatrix} j' & \lambda & j \\ -q & 0 & q \end{pmatrix}. \tag{3.15}$$

Besides being block diagonal in q, the Gaunt coefficients are also simpler to evaluate than the Percival–Seaton coefficients, reflecting the greater decoupling in body-fixed coordinates.

The (necessarily truncated) expansion of the potential in Legendre polynomials, eq. (3.11), is of course appropriate only for certain classes of molecules. In general, these are molecules whose potentials behave as atom–diatom collision complexes, such as Van der Waals systems. For example the complexes formed by H_2 are usually highly isotropic and can be well represented by only a few terms in expansion (3.11) [51,59]. Similarly, Wormer and co-workers [60,61] have shown that the alkali metal cyanides are Van der Waals-like to the extent that their potentials can be accurately represented using a Legendre expansion.

Conversely, most molecules are not well represented by this expansion. In particular the expansion is singular in the region of the nuclear singularities ($R = r/2$ for AB_2 systems). However methods have been developed which allow the formalism discussed above to be applied to any triatomic potential [20,62]. For any potential, expansion (3.11) can be obtained for each (R, r) to arbitrary accuracy using Gauss–Legendre integration [63]. Thus if one multiplies both sides of equation (3.11) by $P_l(\cos\theta)$ and integrates over $\cos\theta$, recognising the orthogonality of Legendre polynomials gives

$$V_l(R, r) = \frac{2}{2l+1}\int_{-1}^{+1} P_l(\cos\theta) V(R, r, \theta)\, \mathrm{d}\cos\theta. \tag{3.16}$$

This integral can be solved exactly using Gauss–Legendre integration with at least $l+1$ quadrature points [64].

This method of using a general potential has been applied successfully to several species which have highly anisotropic potentials, such as CH_2^+ [20], H_2F^+ and H_2Cl^+ [65], H_3^+ [66–69] and heavy–light–heavy vibrationally bonded systems such as IHI and BrHBr [70]. Recent analysis has shown [71] that this method of performing the integration prior to actually constructing the secular matrix has several advantages. Only $\Lambda + 1$ point integration is required, where Λ is the maximum value of λ, independent of the size of the angular basis being used. Furthermore, the pre-integration leads to considerable savings in the computation required to construct the secular matrix. Finally, terms in the expansion with λ greater than $j + j'$ give zero Gaunt coefficients and hence Λ need be no greater than $2j^{\max}$ for accurate solution of the problem, even for molecules for which the potential expansion is slowly convergent. These savings will be particularly important for polyatomic systems where the time taken for integration can become of critical importance [12,14].

3.3. Radial basis functions

Solution of the close-coupled equations implies by (3.10), or their space-fixed equivalents, have been obtained by two general methods. The equations can either be solved by direct numerical integration or by the use of L^2 radial basis set expansions. The latter gives the secular equation or LC-RAMP (linear combination of radial and angular momentum product functions) [49] procedures.

Several numerical integration procedures have been used to directly solve the close-coupled equations [72–75]. Most of these calculations froze the diatomic bond and concentrated on isotropic Van der Waals complexes, for example ref. [76]. Exceptions to this being a calculation on water by Kidd et al. [77], using the artificial channel method and a recent calculation on ozone by Atabek et al. [78]. Neither of these calculations considered rotationally excited states. The problem of treating a large number of angular channels and the unfrozen diatomic coordinate makes these methods unattractive for general nuclear motion calculations.

The use of radial basis functions to get round this problem was first suggested by Le Roy and Van Kranendonk [51]. This allows the ro–vibrational wavefunction of the ith state of a system to be written

$$\psi_i^{J,M} = \sum_j \sum_{q=-j}^{j} \mathcal{Y}_{j,q}^{J,M}(\theta, \alpha, \beta, \gamma) G_{j,q}^{J,i}(R, r), \tag{3.17}$$

where $G_{j,q}^{J,i}$ is a generalised radial function. In practice, this function is always expanded in terms of one dimensional functions

$$G_{j,q}^{J,i} = \sum_m \sum_n c_{j,m,n}^{J,q,i} r^{-1} X_m(r) R^{-1} X_n'(R), \tag{3.18}$$

where the inverse radial terms remove the r^2R^2 factor from the jacobian of Hamiltonian (2.17).

The $\psi_i^{J,M}$ are thus solutions of the secular problem

$$H\psi_i^{J,M} = E_i^J \psi_i^{J,M}, \tag{3.19}$$

with eigenvalue E_i^J and eigenvector coefficients $c_{j,M,n}^{J,q,i}$, which are obtained by diagonalising the secular matrix whose generalised matrix element can be written

$$\langle \mathcal{Y}_{j,q}^{J,M} X_m X_n' \,|\, H \,|\, \mathcal{Y}_{j',q'}^{J,M} X_{m'} X_{n'}' \rangle. \tag{3.20}$$

Solving the nuclear motion problem in this way mirrors the traditional quantum chemical approach to solving the electronic structure problem [79]. Indeed, some vibrational calculations have featured one-dimensional SCF-like steps prior to the solution of the full (within a given basis) CI problem [21,77,80,81].

An important feature of the secular equation approach is that, for a given potential, its solutions satisfy the variational principle. This means that not only can the accuracy of a particular calculation can be determined by demonstrating convergence, but also one can use the variational nature of the calculation to optimize basis sets for a specific problem.

The earliest calculations using the secular equation method and scattering coordinates used numerical basis functions obtained by solving some model problem by direct numerical integration. Usually the model problem was that implied by neglecting the anisotropic components of the potential expansion (3.11) [51]. While this approach can be highly efficient for selected systems [59], there are a number of problems with its general application. Solution of the model problem does not usually give rise to a complete basis because of the dissociative nature of most potentials. This has lead to the inclusion of artificial walls in the model potential so that functions lying in the continuum can be included [82,83]. More seriously, all the calculations which have used numerical functions to represent the R coordinate have simultaneously frozen the r coordinate. It is difficult to imagine a procedure which represents both radial coordinates numerically being computationally tractable. Finally, calculations on anisotropic molecules have found that the isotropic potential does not always yield good radial basis functions. In particular, if the minimum value of R for the isotropic and full potentials are significantly different then very poor basis sets may result [16,54].

As a response to these problems, Tennyson and Sutcliffe [17,20,47] developed the use of polynomial basis functions to represent the radial coordinates. Their philosophy was to use functions which are known analytic solutions of model one-dimensional vibrational problems and which contain parameters, notionally associated with the model potential, which can be adjusted in a systematic fashion to yield a compact basis set representation of the problem.

A well-known diatomic potential is that due to Morse [84]

$$V(z) = D_e\{1 - \exp[-\beta(z - z_e)]\}^2 - D_e, \tag{3.21}$$

whose normalised solutions can be written

$$\beta^{1/2} N_{n,\alpha} \exp(-y/2) y^{b/2} L_n^\alpha(y), \tag{3.22}$$

where

$$y = A \exp[-\beta(z - z_e)] \tag{3.23}$$

and $N_{n,\alpha} L_n^\alpha(y)$ are normalised associated Laguerre polynomials as defined by Gradshteyn and Ryzhik [85]. The parameters in eqs. (3.21)–(3.23) can be represented in terms of the physical parameters of the potential

$$A = \frac{4D_e}{\beta}, \quad \beta = \omega_e\left(\frac{\mu}{2D_e}\right)^{1/2}, \tag{3.24}$$

where D_e is the dissociation energy, ω_e the energy of the fundamental vibration, μ the reduced mass and z_e the equilibrium separation.

For solutions of the Morse potential (3.21), b equals α, and α, the index on $L_n^\alpha(y)$ in function (3.22), equals $A - (2n + 1)$, where n is the order of the polynomial and the degree of vibrational excitation. As α must be greater than -1, the number of bound states supported by the potential is $A/2$. Conversely, if b is chosen as $(\alpha + 1)$ and α is held constant for all n, then the functions (3.22) form a complete orthonormal set for all n. Tennyson and Sutcliffe [17] thus chose to work with α set to the value of the integer nearest A and $b = \alpha + 1$. These Morse-like functions are in fact a special case of the functions originally proposed by Lanczos for diatomic problems [86].

Basis functions of this type, which allow values for D_e, ω_e and z_e to be chosen and systematically optimised, have been successfully used to represent the nuclear motion in both r and R coordinates for a variety of molecules, and form the basis of program ATOMDIAT [87].

However, as was originally shown by ter Haar [88], the Morse oscillator functions (3.22) do not obey the correct boundary conditions at $z = 0$. This is not a problem for diatomics, and hence the r coordinate, as the strongly repulsive nature of the potential ensures that the wavefunction is vanishinghly small at $r = 0$. This property is often encountered for the R coordinate [17], but there are a class of molecules for which it is necessary to have functions which are well behaved at $R = 0$. These are AB_2 systems with linear or quasi-linear geometries and include molecules such as CH_2^+ [20] and vibrationally bonded species IHI and BrHBr [70].

Solutions of the spherical oscillator problem have the form

$$2^{1/2}\beta^{3/4}N_{n,\alpha+1/2}\exp(-y/2)\,y^{\alpha/2}L_n^{\alpha+1/2}(y), \tag{3.25}$$

where

$$y = \beta z^2, \quad \beta = (\mu\omega_e)^{1/2} \tag{3.26}$$

and where $N_{n,\alpha}L_n^\alpha$, μ and ω_e are all as defined for the Morse potential. These functions have finite amplitude at $R = 0$ when $\alpha = 0$ and are zero at $R = 0$ when $\alpha > 0$. They have been found to give a good representation of (quasi-)linear molecules [20,70], when the parameters α and ω_e are optimised variationally, but to be less efficient for bent molecules than the Morse oscillator-like functions [66]. Program ATOMDIAT2 [62] is based on the use of spherical oscillator functions to represent the R coordinate.

3.4. Symmetry

It is necessary to consider two types of symmetry arising from the nuclear motion problem. Firstly, the parity of a particular ro–vibrational state is a good quantum number in addition to its total angular momentum, J, and the projection of J onto the laboratory z axis, M. Secondly, molecules containing identical nuclei possess well defined symmetry properties with respect to interchange of these nuclei [89]. This symmetry is often identified in terms of molecular point group symmetry of some equilibrium structure, but can be represented more generally in terms of permutations which make no assumptions about geometric parameters.

The symmetry of the rotational wavefunction under inversion can easily be represented by transforming the body-fixed angular basis functions to

$$\begin{array}{lll} 2^{-1/2}\left(\mathcal{Y}_{j,q}^{J,M} + (-1)^p\mathcal{Y}_{j,-q}^{J,M}\right) & q > 0, & p = 0, 1, \\ \mathcal{Y}_{j,q}^{J,M} & q = 0, & p = 0. \end{array} \tag{3.27}$$

Conventionally [90] states with $p = 0$ are labelled e and states with $p = 1$ are labelled f. The total parity of a state is given by $(-1)^{J+p}$.

This transformation factorises the secular problem into e and f blocks which can be constructed and diagonalised separately. In the nomenclature of Bunker [89], these functions span the group $C_s(M)$. The integrals within each block for a given $|q|$ are unchanged, with the exception of the Coriolis coupling term between $q = 0$ and $q = 1$ basis functions in the e block:

$$\langle 2^{-1/2}\left(\mathcal{Y}_{j,1}^{J,M} + \mathcal{Y}_{j,-1}^{J,M}\right) | K_{VR} | \mathcal{Y}_{j,0}^{J,M}\rangle = -2^{1/2}C_{J,0}^{+}C_{j,0}^{+}\frac{\hbar^2}{2\mu_1 v_1^2}. \tag{3.28}$$

It is only this off-diagonal Coriolis term which lifts the degeneracy between the e and f blocks. If all the off-diagonal Coriolis terms are neglected then an extra symmetry is introduced: q

Table 1
Comparison of $J = 1^e$ rotational levels for LiCN [54] and CH_2^+ [47], calculated with and without off-diagonal Coriolis interactions. Results of the full calculations are independent of embedding used. Frequencies, in cm^{-1}, are all relative to the $J = 0$ level of the same vibrational state

Embedding	LiCN			CH_2^+				
		R	Full		***R***		*r*	Full
(v_1, v_2, v_3)	*k*			*k*		Ω		
0 0 0	0	1.16	0.89	0	120.2	0	21.2	14.7
	1	127.58	127.57	1	189.0	1	119.2	118.4
0 2 0	0	1.19	0.92					
	1	115.20	115.18					
0 0 1				0	120.3	0	15.9	17.4
				1	173.7	1	120.3	117.9

becomes a good quantum number and states with $|q| > 0$ are doubly degenerate. For many systems the off-diagonal Coriolis terms are small and these states are nearly degenerate. This has led to the neglect of all off-diagonal Coriolis terms in calculations with $J > 0$ by several authors [34,49,54]. A similar approximation, the so called Centrifugal Sudden Approximation, has often been employed in been scattering calculations [91,92].

Table 1 compares results of a typical calculation where neglect of the off-diagonal Coriolis interactions is a good and a poor approximation. Of course, these Coriolis terms depend strongly on the orientation chosen for the body-fixed axes and their neglect will lead to different results if different embeddings are used [20].

The symmetry of AB_2 systems is easily represented within the atom–diatom coordinate system if the atom is taken to be A and the diatom B_2. As the potential must reflect the full symmetry of the molecule, it is invariant with respect to interchange of the identical nuclei. This causes all odd terms in the Legendre expansion (3.11) to be zero for AB_2 systems. In turn, this decouples basis functions which have odd j from those with even j, as the Gaunt coefficient is zero unless $j + \lambda + j'$ is even [55]. States which are symmetric with respect to interchange of two identical nuclei are carried by the j even basis functions, and those which are antisymmetric are carried by j odd. Table 2 classifies the angular basis functions according to the permutation-inversion group $C_{2v}(M)$ which is appropriate for AB_2 systems.

An interesting problem arises when this symmetry is broken by isotopic substitution of one of the like nuclei [63]. In this case the potential retains the AB_2 symmetry, but the kinetic energy operator does not. Usually the symmetry of the potential is broken by the need to define a new coordinate frame which represents the changed position of the molecular centre of mass. For molecules with symmetry related double minima in their potentials, the resulting equilibrium R values for the minima in the asymmetric isotopomer case may be very different, making it difficult to find suitable basis functions to describe both structures simultaneously. An example of this was encountered recently by Farantos and Tennyson when studying H_2^+He [93] and HD*He [94].

Table 2
Classification of the ro–vibrational basis functions according to the irreducible representation of groups $C_{2v}(M)$ and $D_{3h}(M)$ as defined in Appendix I of ref. [89]

Parity of j	Rotational parity	$C_{2v}(M)$	$D_{3h}(M)$
even	$J+p$ even	A_1	A'_1 or E'
even	$J+p$ odd	A_2	A'_2 or E'
odd	$J+p$ odd	B_1	A''_1 or E''
odd	$J+p$ even	B_2	A''_2 or E''

Triatomics with three identical nuclei, A_3 systems, present a particular problem within a method relying on atom–diatom collision coordinates. The appropriate permutation-inversion group for these systems is $D_{3h}(M)$. While the Hamiltonian still retains the full symmetry of the system, it is obscured by the choice of coordinates and it is not easy to adapt the combined angular and radial basis functions to ones belonging to the appropriate irreducible representations. This problem, in relation to H_3^+, has been discussed in detail in an appendix to ref. [66]. Table 2 gives the classification of the ro–vibrational basis functions according to the $D_{3h}(M)$ group. Hyperspherical harmonics appear to represent the easiest way of obtaining full symmetrisation for anharmonic A_3 systems with large amplitude vibrational modes [95,96].

3.5. Basis set selection

Most calculations using scattering coordinates have taken multidimensional basis sets which are simply the combination of all possible one dimensional functions. An exception being the calculation of Kidd et al. [77] who used linear combinations of Legendre polynomials (free rotor functions) to give a "hindered rotor" basis set for their calculations on water.

The problem with using an unrestricted product of one-dimensional basis functions is that as the dimensionality of the problem is increased the basis set becomes increasingly dominated by products of functions with high quantum numbers which give a (negligibly) small contribution to the low lying levels of interest. This problem has naturally received most intense interest from workers performing 6 dimensional tetra-atomic calculations. Criteria tested including using all basis functions such that

$$N^{\max} \geqslant \sum_i n_i/d_i, \tag{3.29}$$

or

$$E^{\max} \geqslant \sum_i n_i \omega_i, \tag{3.30}$$

where mode i has quantum number n_i and fundamental frequency ω_i, and the parameter d_i is introduced to weight lower frequency modes. A mixture of these excitation and energy criteria was found to give the most satisfactory results for formaldehyde [14].

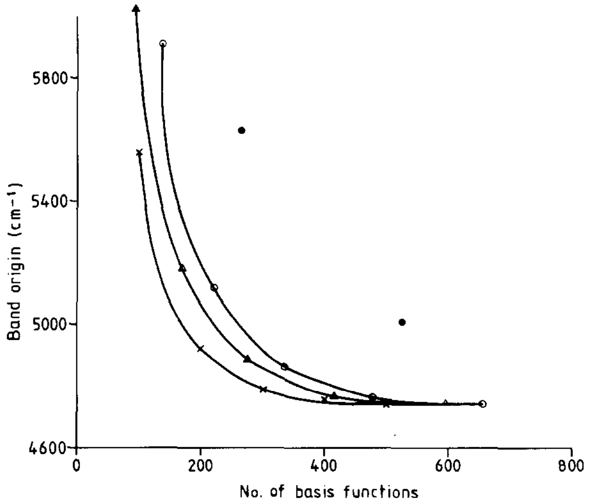

Fig. 2. Convergence of the tenth band origin of HCN as a function of basis set size for several methods of basis set selection [97]. ● simple product basis. △ quantum number selection with $d_j = 4$, ○ quantum number selection with $d_j = 5$. × energy selection criterion.

The scattering coordinates discussed in this article do not lend themselves so naturally to these selection criteria as they do not necessarily correspond to normal modes of the system. However similar method have recently been tested for calculations on HCN [97]. Sample results are given in fig. 2.

The methods tested include the use of simple product one-dimensional sets (as before), the use of quantum number selection criteria (3.29) with special weighting for the low frequency bending mode and the selection of basis functions by excitation energy. The latter method can be regarded as being based on first order perturbation theory and uses the energy of the diagonal elements of the hamiltonian as a selection criterion. It can thus be regarded as a more rigorous form of the energy selection criterion (3.30). As shown by fig. 2 this criterion appears the most promising.

There is still room for more development in this area: in particular a combination of one-dimensional or SCF-like calculations and basis set selection should lead to more compact basis set representations which are vital if highly excited states or polyatomics are to be considered routinely. The extension of basis set selection procedures to make use of second-order perturbation theory which has been used successfully for configuration selection in electronic configuration interaction calculations would be desirable. However, the need for a number of eigenvalues and the general lack of diagonal dominance of the eigenvectors makes such a procedure difficult to implement.

3.6. Rotationally excited states

With the symmetrisation of the rotational functions outlined in section 3.4, the secular matrix factorises into two blocks whose dimensions are proportional to J and $J+1$. As J increases this rapidly leads to secular matrices which are too large to be handled without additional approximations. Approximations used include the neglect of off-diagonal Coriolis interactions, as discussed above, and truncation of the vibrational basis to allow space for the rotational functions [66–68]. Even with the latter approximation, no coupled ro–vibrational calculation with $J > 4$ has been attempted.

Recently, Tennyson and Sutcliffe [98] have used an alternative method for treating the problem of rotationally excited states. It is based upon the secondary variational principle which is well known in solid state physics [99]. The idea is to expand solutions of the full rotational problem in terms of vibrational basis functions which themselves are solutions of a problem for which Coriolis interaction have been neglected.

If one neglects the off-diagonal Coriolis terms, the matrix elements for the resulting vibrational problem can be written

$$\begin{aligned}\langle m, n, j, q \,|\, H \,|\, m', n', j', q'\rangle = {} & \delta_{q,q'}\delta_{j,j'}\delta_{n,n'}[\langle m \,|\, K_r \,|\, m'\rangle + j(j+1)\langle m \,|\, R_r \,|\, m'\rangle] \\ & + \delta_{q,q'}\delta_{j,j'}\delta_{m,m'}[\langle n \,|\, K_R \,|\, n'\rangle + j(j+1)\langle n \,|\, R_R \,|\, n'\rangle] \\ & + \delta_{q,q'}\delta_{j,j'}\delta_{x,x'}[J(J+1) - 2q^2]\langle y \,|\, R_y \,|\, y'\rangle \\ & + \delta_{q,q'}\langle m, n, j, q \,|\, V \,|\, m', n', j', q\rangle, \end{aligned} \tag{3.31}$$

where

$$x = m, \quad y = n, \quad R_y = R_R, \tag{3.32}$$

for the $\boldsymbol{R}$ embedding, and

$$y = m, \quad x = n, \quad R_y = R_r, \tag{3.33}$$

for the $\boldsymbol{r}$ embedding. The kinetic energy operators are given by

$$K_z = -\frac{\hbar^2}{2\mu_z z}\frac{\partial^2}{\partial z^2}z, \quad R_z = \frac{\hbar^2}{2\mu_z z^2}, \quad z = R, r; \quad \mu_R = u, \quad \mu_r = \mu_d. \tag{3.34}$$

Eigenvectors of each secular matrix, for which q is a good quantum number, with eigenvalue $E_i^{J,q}$, can be written

$$\phi_i^{J,q} = \sum_j \sum_m \sum_n c_{j,m,n}^{J,q,i} \mathcal{Y}_{j,q}^{J,M}(\theta, \alpha, \beta, \gamma) r^{-1} X_m(r) R^{-1} X_n'(R). \tag{3.35}$$

If the lowest N_{vib} vibrational functions from each vibrational problem are used to expand the full hamiltonian, one obtains a ro–vibrational secular problem of dimension $N_{\text{vib}}(J+1-p)$. Matrix elements for this problem are given by

$$\begin{aligned}\langle i, q \,|\, H \,|\, i', q'\rangle = {} & \delta_{i,i'}\delta_{q,q'}E_i^{J,q} \\ & - \delta_{q',q+1}(1+\delta_{q,0})^{1/2} C_{J,q}^{+} \langle i, q \,|\, R_z^{+} \,|\, i', q'\rangle \\ & - \delta_{q',q-1}(1+\delta_{q',0})^{1/2} C_{J,q}^{-} \langle i, q \,|\, R_z^{-} \,|\, i', q'\rangle, \end{aligned} \tag{3.36}$$

where for the **R** embedding, $z = R$ and

$$\langle i, q \,|\, R_R^{\pm} \,|\, i', q' \rangle = \sum_j C_{j,q}^{\pm} \sum_m \sum_n \sum_{n'} c_{j,m,n}^{J,q,i} c_{j,m,n'}^{J,q',i'} \langle n \,|\, R_R \,|\, n' \rangle \tag{3.37}$$

and for the **r** embedding, $z = r$ and

$$\langle i, q \,|\, R_r^{\pm} \,|\, i, q' \rangle = \sum_j C_{j,q}^{\pm} \sum_n \sum_m \sum_{m'} c_{j,m,n}^{J,q,i} c_{j,m',n}^{J,q',i'} \langle m \,|\, R_r \,|\, m' \rangle . \tag{3.38}$$

Experience has shown that only a fraction of the full set of vibrational solutions are needed to obtain well converged rotational states for the low-lying vibrational states of the system. This means that not only can calculations be performed for a much greater range of rotational levels, states with J up to 20 have been analysed for H_2D^+ [98], but also there is no need to truncate the basis used to carry the underlying vibrational motions. The algorithm forms the basis of computer program ROTLEV [100].

Table 3 shows the results of a full calculation on the low-lying $J = 1^e$ states of KCN. For comparison "exact" results, i.e. those obtained by direct diagonalisation of the full 475 dimensional ro–vibrational problem, and "No Coriolis" results, i.e. those obtained by treating q as a good quantum number, are also given. Results are shown for both **R** and **r** embeddings. Convergence is satisfactory in both cases, but significantly better for the **R** embedding. This is

Table 3
Convergence of the low-lying $J = 1^e$ levels with number of vibrational basis functions, N_{vib}. The "exact" calculation is that given in Table IV of ref. [17]. Frequencies, in cm^{-1}, are given relative to the $J = 0$ level of each vibrational state.

	N_{vib}		Vibrational state [a]					
			(0, 0)		(0, 1)		(0, 2)	
R embedding		$k =$	0	1	0	1	0	1
No Coriolis			0.299	2.335	0.293	2.581	0.286	2.987
	1		0.298	2.336				
	3		0.289	2.326	0.285	2.575	0.301	3.005
	5		0.288	2.325	0.284	2.573	0.282	2.982
	10		0.288	2.325	0.282	2.571	0.277	2.977
Exact			0.288	2.325	0.282	2.571	0.277	2.977
r embedding		$\Omega =$	0	1	0	1	0	1
No Coriolis			3.899	2.335	3.899	2.851	3.899	2.987
	5		0.315	2.352	0.550	2.832	1.238	3.899
	10		0.291	2.327	0.291	2.578	0.362	3.079
	15		0.288	2.325	0.286	2.573	0.282	2.987
	20		0.288	2.325	0.284	2.571	0.279	2.983
	25		0.288	2.325	0.284	2.571	0.278	2.982
Exact			0.288	2.325	0.282	2.571	0.277	2.977

[a] Vibrational states are labelled (stretch, bend).

because k, unlike Ω, is a nearly good quantum number as can be seen from the calculations which neglected off-diagonal Coriolis interactions.

Chen et al. [4] have recently used a secondary variational method to perform calculations at intermediate rotational excitation ($J \leqslant 10$). They used vibrational functions produced from a $J = 0$ calculation performed using the Whitehead–Handy method [7,8]. This means, that all allowance for centrifugal distortion is carried by the rotational part of the calculation. Their results for the water molecule are impressive, although there is evidence from diatomic calculations that the $J = 0$ vibrational levels do not make such a satisfactory basis when centrifugal distortion effects become large. A similar procedure has recently been used by Spirko et al. for low-lying rotational states, with $J \leqslant 4$, of H_3^+ [101].

It is interesting to ask a priori which embedding will give the best results for a particularly system. Clearly one's aim is to minimize the off-diagonal terms in (3.36). Qualitatively, one can analyse the behaviour of these coupling terms by looking at the operators R_R and R_r of (3.34). The ratio of these is given by

$$\frac{R_R}{R_r} = \frac{2\mu_d r^2}{2\mu R^2} = \frac{m_1(m_2+m_3)^2 r^2}{m_2 m_3(m_1+m_2+m_3)R^2}. \tag{3.39}$$

If $R_R \gg R_r$, then the $\boldsymbol{r}$ embedding is to be prefered and Ω will be the better quantum number, if $R_r \gg R_R$, then the $\boldsymbol{R}$ embedding and k are preferable. Thus, for example, molecules with small values of R will strongly favour the $\boldsymbol{r}$ embedding – see the results for the near linear CH_2^+ molecules given in table 1. Analysis of the available calculations shows that the ratio (3.39) correctly predicts the prefered embedding in all cases.

4. Computational procedures

4.1. Radial matrix element evaluation

Once the angular integration over the potential has been performed, see section 3.2, all the angular matrix elements can be constructed analytically. This leaves the problem of integrating over the radial coordinates, R and r.

For both the Morse oscillator-like functions and the spherical oscillators, the matrix elements of the differential term in the kinetic energy operator can be evaluated analytically. For the Morse-oscillator like functions, with $z = R$ or r *

$$\left\langle n \left| \frac{1}{z}\frac{\partial^2}{\partial z^2} z \right| n' \right\rangle = \frac{\beta^{1/2}}{4}\left\{ \delta_{n,n'}[2n(\alpha+n+1)+\alpha+1]^{1/2} \right.$$
$$- \delta_{n,n'+2}[(\alpha+n)(\alpha+n-1)n(n-1)]^{1/2}$$
$$\left. - \delta_{n,n'-2}[(\alpha+n+2)(\alpha+n+1)(n+2)(n+1)]^{1/2} \right\} \tag{4.1}$$

---

* Note that there is a sign error in the off-diagonal term of eq. (45) of ref. [17] and eq. (11) of ref. [87].

and for the spherical oscillator functions [62]

$$\left\langle n\left|\frac{1}{z}\frac{\partial^2}{\partial z^2}z\right|n'\right\rangle=\frac{\beta^{1/2}}{2}\left\{\delta_{n,n'}(2n+\alpha+3/2)+\delta_{n,n'+1}[n(n+\alpha+1/2)]^{1/2}\right.$$
$$\left.+\,\delta_{n,n'-1}[(n+1)(n+\alpha+3/2)]^{1/2}\right\}+\langle n|z^{-2}|n'\rangle, \tag{4.2}$$

where for the spherical oscillator functions, the integral over the rotational kinetic energy operator z^{-2} can also be obtained analytically [62]

$$\langle n|z^{-2}|n'\rangle=\frac{\beta^{1/2}}{2}\left[\frac{n!}{n'!}\,\frac{\Gamma(n'+\alpha+3/2)}{\Gamma(n+\alpha+3/2)}\right]^{1/2}\sum_{\sigma=0}^{n'}\frac{\Gamma(\sigma+\alpha+1/2)n'!}{\Gamma(n'+\alpha+3/2)\sigma!}\qquad n'\leqslant n \tag{4.3}$$

For both types of radial basis functions the potential matrix elements must be evaluated numerically, as must the z^{-2} integral for the Morse oscillator-like functions. This is efficiently done using M-point Gauss–Laguerre quadrature based on L_M^α where α is the same index as that used in the basis functions. A program for computing such points and weights has been given by Stroud and Secrest [64], but, because of underflow problems, is only reliable for $\alpha < 30$. As, especially for the Morse-like functions, α is often optimally found to have a value of several hundred (it is approximately the number of bound stretching states supported by the potential), it was found necessary to adjust this algorithm [17]. This was done by constructing the integral between *normalised* associated Laguerre polynomials and transferring the factor $\Gamma(M+\alpha+1)$ from the formula for the weights to the normalisation constants of the associated Laguerre polynomials involved in the integral. This gives new formulae for weights and normalisation constants [17,87]

$$w_i'=M!\left[\frac{\mathrm{d}L_M^\alpha(x_i)}{\mathrm{d}x}L_{M-1}^\alpha(x_i)\right]^{-1}, \tag{4.4}$$

$$N_{n,\alpha}'=\left[n!\,\frac{\Gamma(M+\alpha+1)}{\Gamma(n+\alpha+1)}\right]^{1/2}=N_{n,\alpha}[\Gamma(M+\alpha+1)]^{1/2} \tag{4.5}$$

and leaves the position of the quadrature points, $\{x_i\}$, unaltered. This reformulation groups all factorials dependent on α as ratios which can then be evaluated as numerically more stable binomial coefficients.

The radial integral over the potential can now be written

$$\langle m,n|V_\lambda(R,r)|m',n'\rangle=N_{m,\alpha}'N_{m',\alpha}'N_{n,\alpha}'N_{n',\alpha}'\sum_{i=1}^{M}\sum_{j=1}^{M'}w_i'w_j'L_m^\alpha(x_i)L_{m'}^\alpha(x_i)L_n^\alpha(x_j)$$
$$\times L_{n'}^\alpha(x_j)V(x_i,x_j), \tag{4.6}$$

where the quadrature points $\{x_i\}$ and $\{x_j\}$ are related to R and r by equations (3.23) and (3.26) for Morse oscillator-like and spherical oscillator functions respectively. Exact integrals can be obtained in this fashion if $M > m + m'$ and $M' > n + n'$ [71], although experience has shown that $M = m + 3$ and $M' = n + 3$ is usually sufficient [17].

The z^{-2} kinetic energy matrix element between Morse oscillator-like functions can be evaluated similarly

$$\langle n \,|\, z^{-2} \,|\, n' \rangle = N'_{n,\alpha} N'_{n',\alpha} \sum_{i=1}^{M} w'_i L_n^{\alpha}(x_i) L_{n'}^{\alpha}(x_i) \left[z_{\mathrm{e}} + \beta^{-1} \ln(A/x_i) \right]^{-2}, \tag{4.7}$$

where $z = R$ or r.

4.2. Construction of the secular matrix

The time taken to diagonalise the secular matrix is unavoidably determined by the size of the basis set. It is desirable to write the secular matrix construction step such that the rate limiting step is the matrix diagonalisation. This can, with care, be achieved for all programs discussed in this work, provided the potential function is not so complicated that its evaluation becomes rate-limiting.

In the previous sections we have dealt with the evaluation of the matrix elements needed to construct the secular matrix. The radial matrix elements required for the secular matrix element are: the isotropic $\langle m, n \,|\, V_0 \,|\, m', n' \rangle$ and anisotropic $\langle m, n \,|\, V_\lambda \,|\, m', n' \rangle$ potential terms, the vibrational kinetic energy terms $\langle m \,|\, K_r \,|\, m' \rangle$ and $\langle n \,|\, K_R \,|\, n' \rangle$, and the rotational kinetic energy terms $\langle m \,|\, R_r \,|\, m' \rangle$ and $\langle n \,|\, R_R \,|\, n' \rangle$. All of these are precomputed. For maximum efficiency the secular matrix is then constructed in blocks labelled by specific j, q and j', q' values which contain all possible m, n and m', n'; this minimizes the number of Gaunt coefficients that need to be calculated. This algorithm, which is given schematically in fig. 3, was not used originally for ATOMDIAT [87] or ATOMDIAT [62] where matrix construction can become rate-limiting with a fast (vectorised) diagonaliser. Table 4 gives illustrative timings for the different procedures.

When solving the rotational problem using the secondary variational method, see section 3.6, the only matrix elements required are $\langle m \,|\, R_r \,|\, m' \rangle$ or $\langle n \,|\, R_R \,|\, n' \rangle$ according to the embedding chosen. These are passed from the driving vibrational program together with the eigenvalues and eigenvectors of the Coriolis decoupled vibrational problems.

Again, when constructing the secular matrix, the outer loop is taken over q. In the case where $q = q' + 1$, for which the off-diagonal elements are non-zero the matrix elements $\langle i, q \,|\, R_z^{\pm} \,|\, i', q' \rangle$, see eqs. (3.37) or (3.38), are constructed with the loop over j, m, n and n' or j, n, m and m' running outside those on i and i'. This minimizes the amount of testing that needs to be performed and allows the inner loops to vectorise, see fig. 4. This method of construction means that only two sets of coefficients. $c_{j,m,n}^{J,q,i}$, with neighbouring q values are needed in fast memory simultaneously.

4.3. Diagonalisation

The real symmetric matrices generated by this approach have several common characteristics. They are of medium size, bigger than the small ($n < 200$) matrices which can be easily handled in

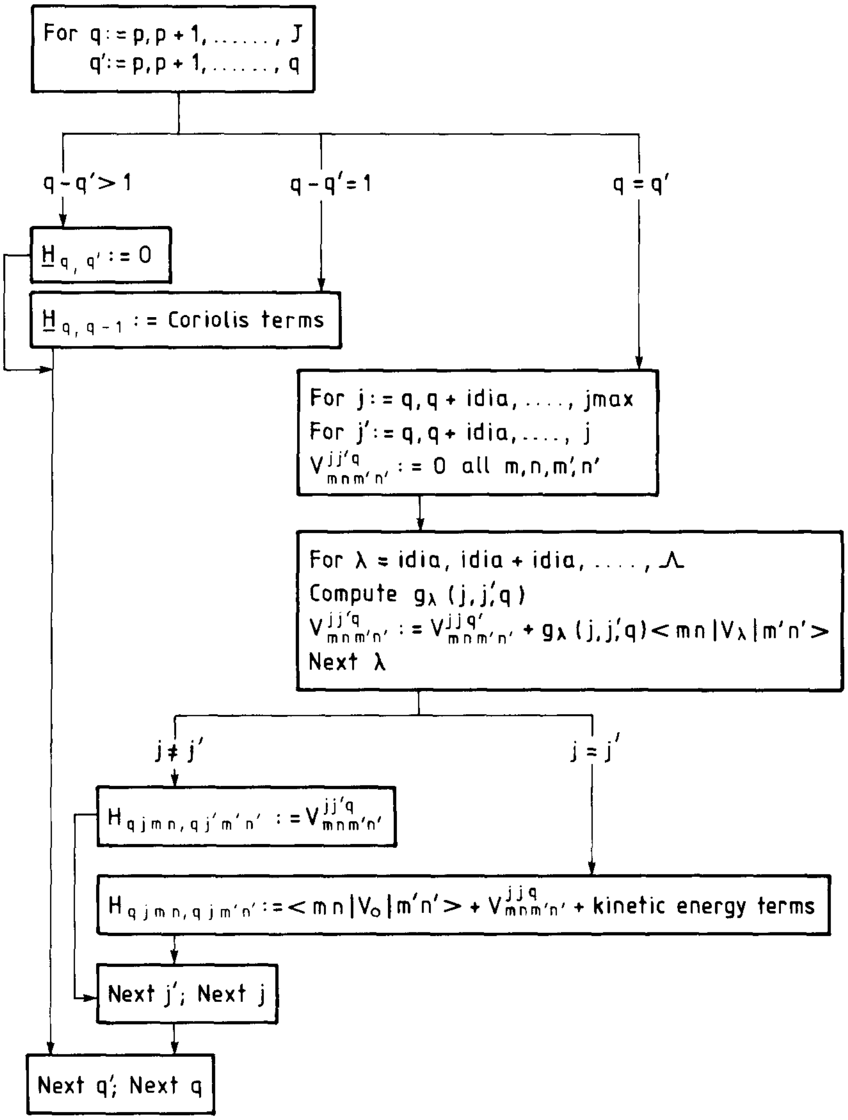

Fig. 3. Algorithm for the construction of the ro-vibrational Hamiltonian matrix. $j^{\max}$ is the maximum value of j in the angular basis set and idia = 1 for a heteronuclear and = 2 for a homonuclear diatomic. Other symbols are as defined in the text.

limited fast memory, and considerably smaller than the very large matrices often encountered in quantum chemical configuration interaction or nuclear physics shell model calculations, which cannot be retained in core and for which the lowest eigenvalue(s) is (are) obtained iteratively. The ro-vibrational matrices are not diagonally dominant, except possibly for certain, highly isotropic Van der Waals complexes. They are not sparse, with, in general, no zero matrix elements for calculations with $J = 0$ or which neglect off-diagonal Coriolis interactions. One usually requires only the s lowest eigenvalues and eigenvectors of the n-dimensional problem, where s is typically less than 50, and n greater than 200.

Table 4
Sample timings for solving a $J = 0$, $m \leqslant 4$, $n \leqslant 6$ and j (even) $\leqslant 18$ problem for CH_2^+ [47]. This gives a 350 dimensional secular problem

Program	Computer	CPU time (s)
ATOMDIAT2	NAS7000 [a]	253.27
ATOMDIAT2	CRAY-1	27.38
ATOMDIAT2 + vectorised diagonaliser [102]	CRAY-1	8.43
As above + optimised secular matrix construction	CRAY-1	3.16

[a] The scalar speed of the CRAY-1 is about 6 times that of the NAS7000.

By performing calculations using the secular matrix method, experience has been acquired on diagonalisation procedures. Initial attention focused on the performance of scalar machines with limited storage [47]. The traditional Householder tridiagonalisation procedure followed by a bisected Sturm sequence [103] was the most satisfactory when the matrix could be retained in fast memory. Several methods of iterative diagonalisation were explored, with the conclusion that an orthogonalised, as opposed to Paige-style, Lanczos algorithm [104] was best suited to this particular problem as it only requires one vector-matrix multiplication per iteration in contrast to Shavitt's method of optimal relaxation [105,106] which required s such operations. This method was thus implemented as an alternative to in core diagonalisation in ATOMDIAT [87]. It should be noted that Davidson's procedure [107], which is similar to the Lanczos algorithm, was not tested.

The advent of fast computers with large or virtual memory and vector or array processing capacity has shifted attention towards algorithms which take advantage of these features. For example, in order to utilize vectorisation potential it is necessary to reformulate the problem in square matrices, rather than the storage saving triangular form. Table 4 illustrates the timing advantage that can be gained by using the computer architecture, in this case the CRAY-1.

The secular matrices generated in the second stage of the secondary variational procedure have rather different properties from those generated in the first stage and discussed above. The matrices become increasingly sparse with increasing J and have a banded structure. Fig. 5 shows the structure of such a matrix.

Three types of diagonalisation have been tried for these matrices [98]: full matrix diagonalisation, banded matrix diagonalisation and an iterative procedure appropriate for sparse matrices [108]. These methods have very different storage requirements which is an important consideration as storage often limits the size of a ro-vibrational calculation more than CPU time. There are $N_{\mathrm{vib}}(N_{\mathrm{vib}} + 1)(J - p) - N_{\mathrm{vib}}^2$ unique, non-zero elements in the secular matrix. Only this number of storage locations are needed for the iterative method for which it is not necessary to store pointers to the non-zero matrix elements as this can be taken care of algorithmically. Banded matrix techniques require approximately twice as many storage locations, $N_{\mathrm{vib}}(2N_{\mathrm{vib}} + 1)(J - p + 1)$, as the band of non-zero elements extends $2N_{\mathrm{vib}}$ places from the diagonal. Retaining the full matrix in core requires approximately J times more storage then the minimum.

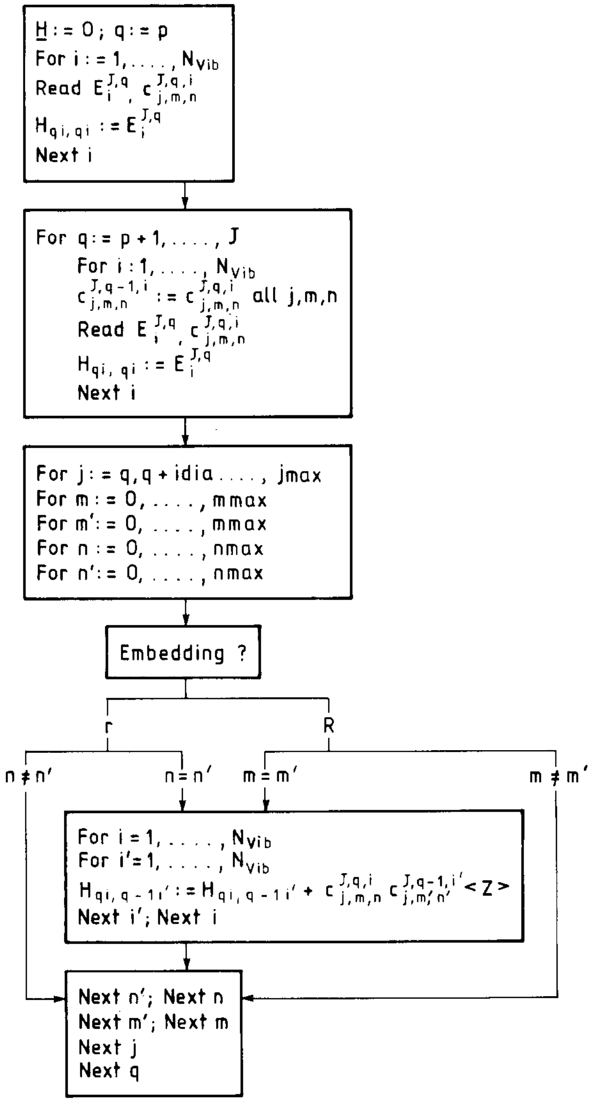

Fig. 4. Algorithm for the construction of the hamiltonian matrix for the second variational step. $j^{\max}$, $m^{\max}$, $n^{\max}$ are the maximum values of j, m and n in the θ, r and R basis sets respectively. idia = 1 for a hetronuclear and = 2 for homonuclear diatomic. $\langle z \rangle = C^{\pm}_{J,q}\langle m \,|\, R^{\pm}_{R} \,|\, m' \rangle$ or $C^{\pm}_{J,q}\langle n \,|\, R^{\pm}_{r} \,|\, n' \rangle$ according to the embedding. Other symbols are as defined in the text.

Test runs have shown that the iterative procedure also is the most economic on CPU time. The reader is referred to ref. [98] for further details.

4.4. Basis set optimisation

The radial basis functions discussed above contain parameters which can be adjusted systematically to give an optimal basis set expansion for a particular calculation. Care has been

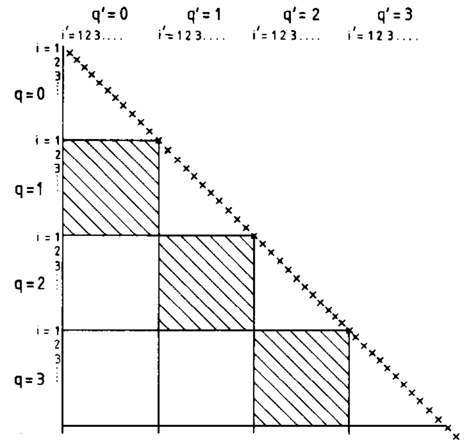

Fig. 5. Structure of the secular matrix for the second stage of a secondary variational calculation. Only the diagonal and shaded areas are non-zero. For a calculation with f parity, remove the blocks with q or $q' = 0$.

taken to relate these parameters to physically defined quantities so that good initial guesses for the parameters can be made. Even so it is usually necessary to adjust the parameters; in particular the optimum value for R_e and r_e used for the Morse oscillator-like functions has consistently been found to be greater than that suggested by the location of the minimum in the potential energy surface. Conversely, the results tend to be insensitive to D_e. Particular case must be taken with the optimisation if a compact basis set representation is required.

When the triatomic potential is well represented, to a first approximation, by an atom–diatom system, the r_e functions used to represent the diatomic coordinate can be optimised for a calculation on the separate diatom species. Experience with HF [47], HCl [45] and CN$^-$ [98] has shown the Morse-like functions to be particularly efficient at representing these diatomic vibrational states; an example is given in table 5. In such cases, the R functions may also be optimised using a 2-D calculations which freezes the r coordinate.

Table 5
Comparison of an optimised 5 ($n \leqslant 4$) Morse oscillator-like function basis representation of the lowest 3 states of HF with the exact results for the empirical potential of Huffaker [109].

	Basis (cm^{-1})	Exact [a] (cm^{-1})
Ground state		
Absolute energy	−47757.74	−47757.78
Rotational constant	20.7055	20.7050
First excited state		
Band origin	3975.93	3975.66
Rotational constant	19.9278	19.9236
Second excited state		
Band origin	7779.10	7777.73
Rotational constant	19.1373	19.1610

[a] Exact results obtained by direct numerical integration [1].

Table 6
Optimisation of 4 ($n \leqslant 3$) Morse oscillator-like functions for a harmonic CN potential [38]

R_e/a_0	D_e/E_h	ω_e/E_h	$v = 0$ (cm^{-1})	$v = 1$ (cm^{-1})
2.4	0.1	0.007	−35734.7	−32442.1
–	–	0.008	45.5	643.1
–	–	0.009	49.3	750.3
2.42	–	–	49.0	755.6
–	0.09	–	49.6	757.7
–	0.08	–	49.0	769.3
–	0.07	–	49.4	753.4
2.44	0.08	–	49.8	767.1
–	–	0.0085	48.5	719.7
–	–	0.0095	50.4	799.8
–	–	0.010	50.65	811.9
–	–	0.011	0.69	50.1
–	0.085	–	0.69	52.2
–	0.09	–	0.70	54.1
–	–	0.0115	0.79	57.5
2.45	–	–	0.85	57.6
–	0.095	–	0.84	59.2
–	0.10	–	0.83	60.6
2.46	–	–	0.87	60.5
–	–	0.0118	0.86	62.5
Optimised				
2.465	0.1045	0.0120	−32750.87	−32863.70

For molecules for which the atom–diatom separation is poor, such as H_3^+ [66], basis functions must be optimised using a full 3-D calculation. This is usually done with truncated basis sets so that the optimisation can be performed in a (near-) interactive fashion. Table 6 shows the results of a typical optimisation session.

An unsatisfactory aspect of the spherical oscillator functions is that they usually require different parameters for different rotationally excited states [20]. This can prove a problem for heavy systems with small rotational constants as the rotational transition frequency can become comparable to the error caused by differing rates of convergence for different states. This is especially true as it has generally proved too expensive to optimise basis sets for rotationally excited states [20,70].

5. Applications

5.1. Weakly bound or Van der Waals complexes

The procedures discussed above have been used for calculations on a variety of triatomic Van der Waals complexes from the highly isotropic NeH_2 molecule [17] to the anisotropic (quantum choatic) ArHCl molecule [45]. Table 7 compares the results of three calculations on NeH_2 using

Table 7
Binding energies (in cm^{-1}) of the bound para-H_2Ne states calculated (1) using ATOMDIAT [17], (2) by Le Roy and Van Kranendonk [51], and (3) using the vector model [111], for which l is a good quantum number

J	l	(1)	(2)	(3)
0	0	4.67	4.70	4.66
1	1	3.52	3.56	3.51
2	2	1.30	1.36	1.30

different methods for the same empirical potential, that of Andreas et al. [110]. The vector model assumes that l, the angular momentum of $\boldsymbol{R}$, is a good quantum number and was used by Waaijer et al. to invert their experimental hyperfine spectra [111]. All three methods give very similar results. The success of the vector model illustrates the ease with which hydrogenic Van der Waals complexes can be treated. This has lead to the development of very quick and accurate methods for the treatment of these systems [112] with a view to least squares fitting to observed transitions.

Conversely there are relatively few calculations which explicitly allow for the coupling of monomer and complex vibrational modes in more anisotropic atom–diatom Van der Waals complexes. Full 3-D calculations have been performed on HeHF [47] and ArHCl [45] using ATOMDIAT, which has the advantage that the polynomial basis sets allow both stretching modes to treated simultaneously. The latter calculation showed an extreme sensitivity to the HCl bondlength and hence vibrational motion, although further analysis suggests that these effects can be accurately accounted for within an adiabatic (Born–Oppenheimer-like) approximation [38].

Recently, Holmer and Certain [113] have used a natural orbital analysis on the wavefunction of model triatomic Van der Waals complexes. This allows the most compact orbital representation to be obtained and has distinct advantages for the assignment of states.

5.2. Strongly bound systems

Although the method of Tennyson and Sutcliffe originally developed from methods designed to treat Van der Waals complexes. It has found greater use as a method of treating more strongly bound triatomics with large amplitude vibrational modes. Several studies have been made which compare the results of these calculations with other methods by using identical potential functions. Example are calculations on KCN [15–17], CH_2^+ [18–22], H_3^+ [66–69,81] and the vibrationally bonded IHI and BrHBr complexes [70]. In all cases ATOMDIAT/ATOMDIAT2, while not necessarily being more efficient than a method designed for a specific class of molecules, gave accurate and reliable results (see, however the discussion at end of section 4.4). Table 8 compares the results of calculations on the H_2F^+ ion obtained using ATOMDIAT [65] with those obtained by Botschwina [114] using the method of Whitehead and Handy [7] and illustrates that this scattering-based procedure can be applied to even fairly rigid molecules.

Of special note among these molecules is H_3^+ and its isotopic variants H_2D^+, HD_2^+ and D_3^+. The electronic simplicity of this system had lead to the calculation of several accurate potential

Table 8
Zero point energy and band origins, in cm^{-1}, for the low-lying levels of H_2F^+ obtained (1) by Botschwina [114] and (2) using ATOMDIAT [65]

(v_1, v_2, v_3)	(1)	(2)
(0, 1, 0)	1373	1374.8
(0, 2, 0)	2681	2690.8
(0, 0, 1)	3315	3314.4
(1, 0, 0)	3355	3355.4
Zero point energy	4157	4157.3

surfaces [115] and extensive comparison with experiment through fitting these surfaces and performing ro–vibrational calculations. Excellent agreement has been found which has aided the interpretation of the complicated empirical spectra [69]. In particular the low lying rotational levels of H_3^+ and the observed vibrational fundamentals of all the species are reproduced with an error of only 0.1% [66,68]. These errors, which can be attributed to small errors in the potential energy surface, are less than some of those given by competing vibrational methods [69], which emphasizes the importance of accurate method for comparison with high resolution experiments. Of the variational methods applied to this problem only Tennyson and Sutcliffe [66–69], using ATOMDIAT, calculated the experimentally important rotationally excited states (more recently this has also been done by Jensen et al. [101,116]) and have since extended this to the challenging problem of the highly excited ($J = 10$–20) rotational levels of H_2D^+. The rotational levels of the system are so widely spaced that the spliting in the $J = 20$ manifold is equivalent to about 10 vibrational spacings [98]. This leads to very strong Coriolis interactions which cannot easily be represented by theories which do not allow for full rotation–vibration coupling.

5.3. Highly excited vibrational states

Highly excited vibrational states are becoming of increased experimental interest. In particular the advent of laser experiments which excite a single vibronic transition and observe its decay into excited states of the ground electronic state ("pump and dump") has made many levels, which were inaccessible by conventional techniques, observable. There have been few quantum mechanical calculations in this area, although those performed using ATOMDIAT on LiCN and KCN, for which the lowest 80 and 30 vibrational states were stabilised respectively, suggest that there is much interesting physics in this region. In particular because of the possible onset of vibrational chaos [44,118,119].

An attempt was also made by Tennyson and Sutcliffe to stabilize many vibrational states of H_3^+ and H_2D^+ [66]. They found that with a basis set limit of 800 functions that the 40th vibrationally excited state in each molecule could only be converged to an accuracy of about 100 cm^{-1}. Although this could be improved by the use of basis selection [69], the scattering coordinates used by Tennyson and Sutcliffe for these calculations are not the natural coordinates for the system. Their experience suggests that for the difficult problem of calculating highly excited states it is necessary to use a method specifically appropriate for the molecular potential under consideration.

5.4. Polyatomic systems

Although the formalism for treating the vibrational levels of a scattering complex formed by two polyatomic molecules has been laid out [48], there have been few applications. This is in part due to the large number of angular degrees of freedom for these systems, but a more severe restriction is the lack of potentials of sufficient accuracy to warrant anything but highly approximate treatments of the nuclear motion problem.

Tennyson and Van der Avoird [49] tackled the nitrogen dimer using an extension of the method of Tennyson and Sutcliffe. They were able to use permutation symmetry to separate the 670 angular channels for the $J = 0$ problem into blocks, the largest of which comprised only 95 channels. However the $(N_2)_2$ potential is comparatively isotropic with only terms with $l \leqslant 6$ in the spherical harmonic expansion used to represent the ab initio data [119]. Conversely, calculations on the argon–tetrazine complex found a highly anisotropic potential requiring many terms in the potential expansion and large angular basis sets to obtain convergence [120].

Strongly bound atom–polyatom systems have also received some attentions. Baranov and Boldyrev performed model calculations on $L{-}MH_4$ ($L = Li$, Na; $M = B$, C^+) using very simple, one parameter, potential functions [121] and $Li{-}MF_4$ ($M = B$, Al) using two parameter potentials [122]. This approach has since been extended to $Na{-}ClO_4$ using a more realistic potential function obtained by inverting empirical solid state data [50]. These calculations all froze the MX_4^- ion in a tetrahedral geometry, Baranov and Boldyrev making the additional approximation that the R coordinate (the L–M separation) was also frozen.

Although few polyatomic calculations have so far been performed, a section on them has been included because undoubtedly they will be an area of future development. The theoretical generalisation of atom–diatom methods to the polyatom–polyatom case has been given [48] and many of the triatomic computational techniques outlined in this article can be directly transferred. As is clear from the limited problems so far tackled [43,49,50,76,121–123], symmetry can be expected to be of increased importance in these polyatomic calculations.

6. Beyond ro-vibrational calculations

6.1. Dipolar properties

While the calculation of ro-vibrational stationary states requires only a knowledge of the potential energy surface many properties also depend on the variation of dipoles with geometry. With a dipole surface one can calculate vibrationally averaged dipoles, infrared and microwave transition intensities, and fluorescence spectra and lifetimes. All of these are, at least in principle, experimentally accessible.

If one is using a potential energy surface expanded in scattering coordinates, eq. (3.11), it is natural to use an analogous expansion to represent the dipole surface. For a triatomic lying in the x–z plane in the dipole surface takes the form

$$\mu_z(R, r, \theta) = \sum_\lambda C_{\lambda,0}(r, R)\Theta_{\lambda,0}(\theta), \tag{7.1}$$

$$\mu_x(R, r, \theta) = \sum_\lambda C_{\lambda,1}(r, R)\Theta_{\lambda,1}(\theta). \tag{7.2}$$

All the dipole properties discussed above depend on the expectation value of this dipole surface with wavefunctions of appropriate ro–vibrational states. It is thus necessary to perform integrals over the dipole surface in a similar fashion to those constructed over the potential function.

Angular integrals over the dipole functions (7.1) and (7.2) can be evaluated analytically [124]:

$$\begin{aligned}\langle \mathcal{Y}^{J,M}_{j,q} \,|\mu_v|\, \mathcal{Y}^{J,M}_{j',q'}\rangle &= (-1)^M[(2J+1)(2J'+1)]^{1/2}\begin{pmatrix} J & 1 & J' \\ -M & v & M' \end{pmatrix} \\ &\times \sum_{v'=-1}^{1} \sum_{\lambda} C_{\lambda,|v'|}\, a(j,\ j',\ \lambda,\ v') \\ &\times b(v'-q)\begin{pmatrix} J & 1 & J' \\ -q & v' & q-v' \end{pmatrix}\begin{pmatrix} j & \lambda & j' \\ -k & v' & k-v' \end{pmatrix}\begin{pmatrix} j & \lambda & j' \\ 0 & 0 & 0 \end{pmatrix},\end{aligned} \tag{7.3}$$

where

$$\begin{aligned} &a(j,\ j',\ \lambda,\ 0) = [(2j+1)(2j'+1)]^{1/2}, \\ &a(j,\ j',\ \lambda,\ \pm 1) = -[(2j+1)(2j'+1)\lambda(\lambda+1)/2]^{1/2}, \\ &b(0) = 2^{-1/2}, \quad b(\neq 0) = 1 \end{aligned} \tag{7.4}$$

and radial integrals can again be performed using Gauss–Laguerre integration.

Dipole surface have been used to generate theoretical spectra for KCN [124], LiCN [124] and the nitrogen dimer [125], as well as for calculating fluorescence lifetimes and spectra [126]. The latter calculation showed that even when the neglect of the off-diagonal Coriolis interactions is a good approximation for the energy levels, it can be a poor approximation for other (dipolar) properties because of the large effect of small amounts of mixing, for instance between forbidden and allowed transitions.

6.2. *Born–Oppenheimer breakdown*

Although there are molecules with large amplitude vibrational modes for which the coupling of potential energy surfaces is known to be important, such as CH_2^+ [27] and C_2H^+ [127], no coupled surface calculations have been performed using scattering coordinates. These have however been used to study fine and hyperfine structure effects caused by the coupling of electron and nuclear spin to the molecular angular momentum. These studies have concentrated on Van der Waals systems for which the (hyper)fine structure of the monomers was well known.

An interesting feature of these Van der Waals (hyper)fine structure effects is that while they are relatively insensitive to the details of the isotropic interaction potential, they provide a sensitive probe of the anisotropic terms in the potential expansion (3.11). This is in contrast to many interaction properties which depend largely on the isotropic potential. Thus Reuss and co-workers [111,128,129] were able to use a simplified version of space-fixed Hamiltonian (2.6), the vector model (see section 5.1), plus hyperfine terms to invert the hyperfine spectra of Van der Waals complexes containing H_2. They were able to significantly improve the anisotropic terms in the available empirical potentials.

The fine structure of the ro–vibrational levels of O_2-rare gas Van der Waals complexes has been studied using an extension of space-fixed Hamiltonian (2.6) [83,130]. In these studies no approximate quantum numbers were assumed as the anisotropic terms in the potential were found to significantly perturb the fine structure spectra. The structure of these spectra has been explained by Van der Avoird [131]. These studies also included a consideration of the first-order Zeeman splitting of the levels due to a weak magnetic field.

7. Concluding remarks

This article has dealt with the computational techniques that have been used to calculate the ro–vibrational spectra of small molecules, particularly triatomics, with one or more large amplitude vibrational mode. Although two of the programs discussed are published, ATOMDIAT [87] and ATOMDIAT2 [62], the majority are not. It is my intention to provide a more flexible program suite [100] for calculating the ro–vibrational levels of triatomic molecules, which, besides unifying ATOMDIAT and ATOMDIAT2, will offer options to allow basis set selection, a choice of embeddings and calculation of rotationally excited states.

Finally, mention should be made of a recent development which has generalised the embeding procedure given in section 2 to give a unified body-fixed Hamiltonian for triatomic molecules. The Hamiltonian depends on the internal coordinates of the molecule expressed as two length and an angle, and a simple parameter which allow one to switch between coordinate representations, with the scattering coordinates used in this article as a special case [132]. Solutions of this Hamiltonian have been obtained for a few trial problems (CH_2^+, D_2H^+, H_2^*He, HD*He) using a generalisation of the numerical procedures given here [132].

Acknowledgements

I am grateful to my various collaborators for letting me use the results quoted here and in particular to Dr. Brian Sutcliffe for his encouragement. I thank Dr. Brian Sutcliffe and Dr. Stavros Farantos for helpful comments on this manuscript. I would also like to express my thanks to the Science and Engineering Research Council in whose Daresbury Laboratory the first draft of this article was written.

References

[1] R.J. Le Roy, J. Chem. Phys. 54 (1971) 5433.
[2] P. Pulay, in: The Force Concept in Chemistry, ed. B. Deb (Van Nostrand, New York, 1981).
[3] B.R. Henry, in: Vibrational Spectra and Structure, vol. 10, ed. J.R. Durig (Elsevier, New York, 1981).
[4] C.-L. Chen, B. Maessen and M. Wolfsberg, J. Chem. Phys. 83 (1985) 1795.
[5] C. Eckart, Phys. Rev. 47 (1935) 552.

[6] G.D. Carney, L.L. Sprandel and C.W. Kern, Advan. Chem. Phys. 37 (1978) 305.
[7] R.J. Whitehead and N.C. Handy, J. Mol. Spectr. 55 (1975) 356.
[8] R.J. Whitehead and N.C. Handy, J. Mol. Spectr. 59 (1976) 459.
[9] J.K.G. Watson, Mol. Phys. 15 (1968) 476.
[10] P. Botschwina, Chem. Phys. 40 (1979) 33.
[11] P. Botschwina, H. Haertner and W. Sawodny, Chem. Phys. Lett. 74 (1980) 459.
[12] S. Carter and N.C. Handy, Chem. Phys. Lett. 79 (1981) 118, 83 (1981) 219.
[13] P. Bopp, D. McLauglin and M. Wolfsberg, Z. Naturforsch. Teil. A 37 (1982) 393.
[14] B. Maessen and M. Wolfsberg, J. Chem. Phys. 80 (1984) 4651.
[15] J. Tennyson and B.T. Sutcliffe, Mol. Phys. 46 (1982) 97.
[16] J. Tennyson and A. van der Avoird, J. Chem. Phys. 76 (1982) 5710.
[17] J. Tennyson and B.T. Sutcliffe, J. Chem. Phys. 77 (1982) 4061.
[18] R. Bartolomae, D. Martin and B.T. Sutcliffe, J. Mol. Spectr. 87 (1982) 367.
[19] S. Carter and N.C. Handy, J. Mol. Spectr. 95 (1982) 9.
[20] J. Tennyson and B.T. Sutcliffe, J. Mol. Spectr. 101 (1983) 71.
[21] S. Carter and N.C. Handy, Mol. Phys. 47 (1982) 1445.
[22] S. Carter, N.C. Handy and B.T. Sutcliffe, Mol. Phys. 49 (1983) 745.
[23] J.K.G. Watson, Mol. Phys. 19 (1970) 465.
[24] N.C. Handy, private communication.
[25] B.T. Sutcliffe, Mol. Phys. 48 (1983) 561.
[26] B.T. Sutcliffe, in: Current Aspects of Quantum Chemistry, ed. R. Carbo, Studies in Theoretical Chemistry, vol. 21 (Elsevier, Amsterdam, 1982) p. 99.
[27] S. Carter and N.C. Handy, Mol. Phys. 52 (1984) 1367.
[28] S. Carter and N.C. Handy, Mol. Phys. 53 (1984) 1033.
[29] A. Sayvetz, J. Chem. Phys. 6 (1939) 383.
[30] P.R. Bunker, Ann. Rev. Phys. Chem. 34 (1983) 59.
[31] P. Jensen, Comput. Phys. Rep. 1 (1983) 1.
[32] P. Botschwina, Chem. Phys. 40 (1979) 33.
[33] S.L. Holmgren, M. Waldman and W. Klemperer, J. Chem. Phys. 67 (1977) 4414.
[34] S.L. Holmgren, M. Waldman and W. Klemperer, J. Chem. Phys. 69 (1978) 1661.
[35] J.M. Hutson and B.J. Howard, Mol. Phys. 41 (1980) 1123.
[36] H. Romanowski and J.M. Bowman, Chem. Phys. Lett. 110 (1984) 235.
[37] J. Makarewicz and A. Wierbicki, J. Mol. Spectr. 108 (1984) 155.
[38] S.C. Farantos and J. Tennyson, J. Chem. Phys. (in press).
[39] A.R. Hoy and P.R. Bunker, J. Mol. Spectr. 52 (1974) 439, 74 (1979) 1.
[40] P. Jensen, P.R. Bunker and A.R. Hoy, J. Chem. Phys. 77 (1982) 5370.
[41] P.R. Bunker and P. Jensen, J. Mol. Spectr. 99 (1983) 348.
[42] J.M. Hutson and B.J. Howard, Mol. Phys. 43 (1981) 493, 45 (1982) 769, 45 (1982) 791.
[43] A.E. Barton and B.J. Howard, Faraday Disc. Chem. Soc. 73 (1982) 45.
[44] J. Tennyson and S.C. Farantos, Chem. Phys. 93 (1985) 237.
[45] J. Tennyson, Mol. Phys. 55 (1985) 463.
[46] A.M. Arthurs and A. Dalgarno, Proc. Roy. Soc. Ser. A 256 (1960) 540.
[47] J. Tennyson and B.T. Sutcliffe, J. Chem. Phys. 79 (1983) 43.
[48] G. Brocks, A. van der Avoird, B.T. Sutcliffe and J. Tennyson, Mol. Phys. 50 (1983) 1025.
[49] J. Tennyson and A. van der Avoird, J. Chem. Phys. 77 (1982) 5664, 80 (1984) 2986.
[50] G. Brocks, J. Tennyson and M. Leslie, work in progress.
[51] R.J. Le Roy and J. Van Kranendonk, J. Chem. Phys. 61 (1974) 4750.
[52] R.J. Le Roy and J.S. Carney, Advan. Chem. Phys. 42 (1980) 353.
[53] V.A. Istomin, H.F. Stepanov and B.I. Zhilinskii, J. Mol. Spectr. 67 (1977) 265.
[54] G. Brocks and J. Tennyson, J. Mol. Spectr. 99 (1983) 263.
[55] D.M. Brink and G.R. Satchler, Angular Momentum, 2nd ed. (Clarendon, Oxford, 1968).
[56] E.U. Condon and G.H. Shortley, The Theory of Atomic Spectra (Cambridge University, Cambridge, 1935).

[57] I.C. Percival and M.J. Seaton, Proc. Cambridge Philos. Soc. 53 (1957) 654.
[58] R.O. Buehler and J.O. Hirschfelder, Phys. Rev. 83 (1950) 628.
[59] J. Tennyson, Chem. Phys. Lett. 86 (1982) 181.
[60] P.E.S. Wormer and J. Tennyson, J. Chem. Phys. 75 (1981) 361.
[61] R. Essers, J. Tennyson and P.E.S. Wormer, Chem. Phys. Lett. 89 (1982) 223.
[62] J. Tennyson, Comput. Phys. Commun. 32 (1984) 109.
[63] W.-K. Liu, J.E. Grabenstetter, R.J. Le Roy and F.R. McCourt, J. Chem. Phys. 68 (1978) 5028.
[64] A.H. Stroud and D. Secrest, Gaussian Quadrature Formulae (Prentice-Hall, London, 1965).
[65] P. Wells and J. Tennyson, unpublished work.
[66] J. Tennyson and B.T. Sutcliffe, Mol. Phys. 51 (1984) 887.
[67] J. Tennyson and B.T. Sutcliffe, Mol. Phys. 54 (1985) 141.
[68] J. Tennyson and B.T. Sutcliffe, Mol. Phys. 56 (1985) 1175.
[69] J. Tennyson and B.T. Sutcliffe, J. Chem. Soc. Faraday Trans. (1986) in press.
[70] S. Carter, D.C. Clary, J.N.L. Connor and J. Tennyson, J. Chem. Phys. (to be submitted).
[71] J. Tennyson, Comput. Phys. Commun. 38 (1985) 39.
[72] A.M. Dunker and R.G. Gordan, J. Chem. Phys. 64 (1976) 4984.
[73] B.R. Johnson, J. Chem. Phys. 69 (1979) 4678.
[74] M. Shapiro and G.G. Balint-Kurti, J. Chem. Phys. 71 (1979) 1461.
[75] G. Danby, J. Phys. B 16 (1983) 3393.
[76] G. Danby and D.R. Flower, J. Phys.B 16 (1983) 3411.
[77] I.F. Kidd, G.G. Balint-Kurti and M. Shapiro, Faraday Disc. Chem. Soc. 71 (1981) 287.
[78] O. Atabek, S. Miret-Artes and M. Jacon, J. Chem. Phys. 83 (1985) 1769.
[79] H.F. Schaefer III, Methods of Electronic Structure Theory (Plenum, New York, 1977).
[80] G.D. Carney and R.N. Porter, J. Chem. Phys. 60 (1974) 4251.
[81] P.G. Burton, E. von Nagy-Felsobuki and G. Doherty, Chem. Phys. Lett. 104 (1984) 323.
[82] R.J. Le Roy, J.S. Carley and J.E. Grabenstetter, Faraday Disc. Chem. Soc. 62 (1977) 69.
[83] J. Tennyson and A. van der Avoird, Chem. Phys. Lett. 105 (1984) 49.
[84] P.M. Morse, Phys. Rev. 34 (1929) 57.
[85] I.S. Gradshteyn and I.H. Ryzhik, Tables of Integrals, Series and Products (Academic, New York, 1980).
[86] C. Lanczos, J. Res. NBS, 45 (1950) 225.
[87] J. Tennyson, Comput. Phys. Commun. 29 (1983) 307.
[88] D. ter Haar, Phys. Rev. 70 (1946) 222.
[89] P.R. Bunker, Molecular Symmetry and Spectroscopy (Academic Press, New York, 1979).
[90] J.M. Brown, J.T. Hougen, K.-P. Huber, J.W.C. Johns, I. Kopp, H. Lefrebvre-Brion, A.J. Merer, D.A. Ramsay, J. Rostos and R.N. Zare, J. Mol. Spectr. 55 (500) 1975.
[91] P.K. Hoffmann, J.W. Evans and D.J. Kouri, J. Chem. Phys. 80 (1984) 144.
[92] R.T. Pack, J. Chem. Phys. 60 (1975) 633.
[93] S.C. Farantos and J. Tennyson, J. Chem. Phys. 82 (1985) 2163 and unpublished work.
[94] S.C. Farantos and J. Tennyson, unpublished work.
[95] J.G. Frey, Chem. Phys. Lett. 102 (1983) 42.
J.G. Frey and B.J. Howard, Chem. Phys. 99 (1986) 415, 427.
[96] P. Bartlett, D. Phil. Thesis, Oxford University (1985).
[97] J. Tennyson and S.C. Farantos, work in progress.
[98] J. Tennyson and B.T. Sutcliffe, Mol. Phys. (in press).
[99] See for example H.J.F. Jansen and A.J. Freeman, Phys. Rev. B 30 (1985) 561.
[100] J. Tennyson, Comput. Phys. Commun. (submitted).
[101] V. Spirko, P. Jensen, P.R. Bunker and A. Cejchan, J. Mol. Spectr. 112 (1985) 183.
[102] Subroutine EIGSFM, B.S. Garbow, J.M. Boyle, J.J. Dongarra and C.B. Moler, Matrix Eigensystem routines – EISPACK Guide Extension, Lecture Notes in Computer Science, Vol. 51 (Springer-Verlag, New York, 1977).
[103] J.M. Ortega, in: Mathematics for Digital Computers, vol. 2, eds. A. Ralston and H.S. Wolf (Wiley, New York, 1967) p. 94.
[104] B.N. Partlett, The Symmetric Eigenvalue Problem, (Prentice-Hall, Englewood Cliffs, N.J., 1980) chap. 13.

[105] I. Shavitt, C.F. Bender, A. Pipano and R.P. Hosteny, J. Comput. Phys. 11 (1973) 90.
[106] R.C. Raffenetti, J. Comput. Phys. 32 (1979) 403.
[107] E.R. Davidson, J. Comput. Phys. 11 (1973) 90.
[108] FO2FJF, NAG Fortran Library Manual, Mark 11, vol. 4 (1983).
P.J. Nikolai, ACM Trans. Math. Software 5 (1979) 118.
[109] J.N. Huffaker, J. Chem. Phys. 64 (1976) 4564.
[110] J. Andreas, U. Buck, F. Huisken, J. Schleusener and F. Torrello, J. Chem. Phys. 73 (1980) 5620.
[111] M. Waaijer, M. Jacobs and J. Reuss, Chem. Phys. 63 (1981) 247.
[112] J.M. Hutson and R.J. Le Roy, J. Chem. Phys. 83 (1985) 1197.
[113] B.K. Holmer and P.R. Certain, J. Phys. Chem. 89 (1985) 4464.
[114] P. Botschwina, in Molecular Ions, eds. J. Berkowitz and K.-O. Groeneveld (Plenum, New York, 1983).
[115] P. Botschwina, W. Meyer and P.G. Burton, J. Chem. Phys. 84 (1986) 891 and references therein.
[116] P. Jensen, V. Spirko and P.R. Bunker, J. Mol. Spectr. 115 (1986) 269.
[117] J. Tennyson and S.C. Farantos, Chem. Phys. Lett. 109 (1984) 165.
[118] S.C. Farantos and J. Tennyson, J. Chem. Phys. 82 (1985) 800.
[119] R.M. Berns and A. van der Avoird, J. Chem. Phys. 72 (1980) 6107.
[120] G. Brocks, private communication.
[121] L.Ya. Baranov and A.I. Boldyrev, Chem. Phys. Lett. 96 (1983) 218.
[122] L.Ya. Baranov and A.I. Boldyrev, Mol. Phys. 54 (1985) 989.
[123] P.R. Bunker, Can. J. Phys. 57 (1979) 2099.
[124] G. Brocks, J. Tennyson and A. van der Avoird, J. Chem. Phys. 80 (1984) 3223.
[125] G. Brocks and A. van der Avoird, Mol. Phys. 55 (1985) 11.
[126] J. Tennyson, G. Brocks and S.C. Farantos, Chem. Phys. 104 (1986) 399.
[127] G. Fogarasi, J.E. Boggs and P. Pulay, Mol. Phys. 50 (1983) 139.
[128] J. Verberne and J. Reuss, Chem. Phys. 50 (1980) 137, 54 (1981) 189.
[129] M. Waaijer and J. Reuss, Chem. Phys. 63 (1981) 263.
[130] J. Tennyson and J. Mettes, Chem. Phys. 76 (1983) 195.
[131] A. van der Avoird, J. Chem. Phys. 79 (1983) 1170.
[132] B.T. Sutcliffe and J. Tennyson, Mol. Phys. (in press).